



New glyme–cyclic imide lithium salt complexes as thermally stable electrolytes for lithium batteries

Takashi Tamura, Takeshi Hachida, Kazuki Yoshida, Naoki Tachikawa, Kaoru Dokko, Masayoshi Watanabe*

Department of Chemistry and Biotechnology, Yokohama National University, 79-5 Tokiwadai, Hodogaya-ku, Yokohama 240-8501, Japan

ARTICLE INFO

Article history:

Received 28 September 2009

Received in revised form

13 November 2009

Accepted 13 November 2009

Available online 16 December 2009

Keywords:

Glyme–Li salt complexes

Room temperature ionic liquid

PGSE-NMR

Oxidative stability

Lithium secondary battery

ABSTRACT

New glyme–Li salt complexes were prepared by mixing equimolar amounts of a novel cyclic imide lithium salt $\text{Li}(\text{C}_2\text{F}_4\text{S}_2\text{O}_4)$ (LiCTFSI) and a glyme (triglyme (G3) or tetraglyme (G4)). The glyme–Li salt complexes, $[\text{Li}(\text{G}3)][\text{CTFSI}]$ and $[\text{Li}(\text{G}4)][\text{CTFSI}]$, are solid and liquid, respectively, at room temperature. The thermal stability of $[\text{Li}(\text{G}4)][\text{CTFSI}]$ is much higher than that of pure G4, and the vapor pressure of $[\text{Li}(\text{G}4)][\text{CTFSI}]$ is negligible at temperatures lower than 100 °C. Although the viscosity of $[\text{Li}(\text{G}4)][\text{CTFSI}]$ is high (132.0 mPa s at 30 °C), because of its high molar concentration (ca. 3 mol dm⁻³), its ionic conductivity at 30 °C is relatively high, i.e., 0.8 mS cm⁻¹, which is slightly lower than that of a conventional organic electrolyte solution (1 mol dm⁻³ LiTFSI dissolved in propylene carbonate). The self-diffusion coefficients of a Li⁺ cation, a CTFSI⁻ anion, and a glyme molecule were measured by the pulsed gradient spin-echo NMR method (PGSE-NMR). The ionicity (dissociativity) of $[\text{Li}(\text{G}4)][\text{CTFSI}]$ at 30 °C is ca. 0.5, as estimated from the PGSE-NMR diffusivity measurements and the ionic conductivity measurements. Results of linear sweep voltammetry revealed that $[\text{Li}(\text{G}4)][\text{CTFSI}]$ is electrochemically stable in an electrode potential range of 0–4.5 V vs. Li/Li⁺. The reversible deposition–stripping behavior of lithium was observed by cyclic voltammetry. The $[\text{LiCoO}_2][\text{Li}(\text{G}4)][\text{CTFSI}]/\text{Li}$ metal cell showed a stable charge–discharge cycling behavior during 50 cycles, indicating that the $[\text{Li}(\text{G}4)][\text{CTFSI}]$ complex is applicable to a 4 V class lithium secondary battery.

© 2009 Elsevier B.V. All rights reserved.

1. Introduction

Lithium ion secondary batteries (LiBs) have been widely used as power sources for portable devices because of their high energy and power density. In conventional LiBs, organic electrolyte solutions consisting of organic solvents, which exhibit flammability and volatility, are used. Development of a safe electrolyte for LiBs is strongly desired for large-scale energy storage systems, such as batteries for electric vehicles [1–3]. For example, solid polymer electrolytes [4,5] and solid inorganic electrolytes [6,7], which would greatly enhance safety, have been intensively investigated. However, thus far, it has been difficult to apply these solid electrolytes to high power density LiBs, because of their low ionic conductivity.

Room temperature ionic liquids (RTILs) have attracted much attention as safe electrolytes for electrochemical devices. RTILs, which are composed entirely of cations and anions, are liquid under ambient temperature. RTILs have unique properties, for exam-

ple, nonflammability, nonvolatility, high ionic conductivity, and high chemical stability. Many researchers are attempting to apply RTILs to electrochemical devices such as lithium secondary batteries [8–25], electric double-layer capacitors [26–28], dye-sensitized solar cells [29,30], and fuel cells [31–34] as thermally stable electrolytes.

Glyme–Li salt complexes are equimolar mixtures consisting of a glyme and a Li salt [35–37]. In suitable combinations, the oxygen atoms in a glyme coordinate with Li⁺ to form a complex cation, as observed in crown ether complexes, in which the Li⁺ cation and the ligand (glyme) serve as Lewis acid and Lewis base, respectively. If the melting points of glyme–Li salt complexes are sufficiently low to keep them liquid at room temperature, it might be assumed that these molten complexes behave like RTILs, consisting of a Li⁺–glyme complex cation and an anion. We have found that certain equimolar mixtures of a glyme and a Li salt have low melting temperatures and exhibit properties similar to those of RTILs. For instance, glyme (triglyme (G3) or tetraglyme (G4))/lithium bis(trifluoromethylsulfonyl)imide (LiTFSI) equimolar complexes are liquid under ambient temperature and have low flammability, low volatility, high lithium ion concentration, and a wide window of electrode potential [38].

* Corresponding author.

E-mail address: mwatanab@ynu.ac.jp (M. Watanabe).

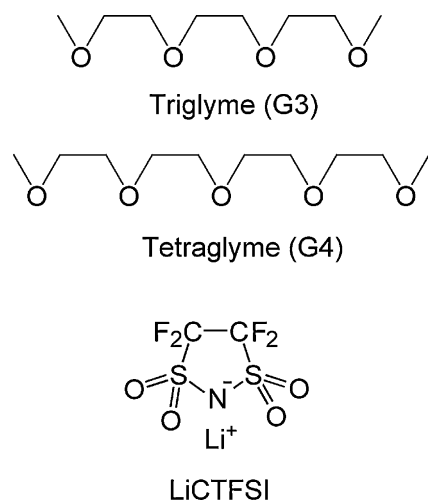


Fig. 1. Chemical structures of glymes and LiCTFSI.

It is of great interest to explore a new lithium salt that forms liquid complexes with glymes and find an applicability to LiBs. In this study, a new cyclic imide salt, lithium 1,2,3-dithiazolidine-4,4,5,5-tetrafluoro-1,1,3,3-tetraoxide $[\text{LiN}(\text{C}_2\text{F}_4\text{S}_2\text{O}_4)]$ (LiCTFSI), was complexed with glymes (G3 or G4) (Fig. 1). The physicochemical properties (ionic conductivity, viscosity, density, and self-diffusion coefficient of chemical species in the eutectic) of $[\text{Li}(\text{G3})][\text{CTFSI}]$ and $[\text{Li}(\text{G4})][\text{CTFSI}]$ were explored. In addition, a $[\text{Li}$ metal] $[\text{Li}(\text{G4})][\text{CTFSI}]/\text{LiCoO}_2$ cell was fabricated, and its charge–discharge performance was evaluated.

2. Experimental

$[\text{Li}(\text{G3})][\text{CTFSI}]$ and $[\text{Li}(\text{G4})][\text{CTFSI}]$ were prepared by simple mixing of glymes (G3 or G4) with LiCTFSI. Distilled and dried triglyme (G3) and tetraglyme (G4) (Kishida Chemical) and LiCTFSI (kindly provided by Asahi Glass) were stored in an argon-filled glove box ($\text{H}_2\text{O} < 1$ ppm, VAC). Equimolar amounts of a glyme (G3 or G4) and LiCTFSI were weighed and mixed in a sample vessel in the glove box. G4 and LiCTFSI were mixed for 24 h at room temperature, and a homogeneous liquid was obtained. In the case of $[\text{Li}(\text{G3})][\text{CTFSI}]$, G3 and LiCTFSI were mixed at 80°C for 24 h, and the obtained liquid was cooled to room temperature. The obtained $[\text{Li}(\text{G3})][\text{CTFSI}]$ was a solid at room temperature.

Differential scanning calorimetry (DSC) was carried out by using a Seiko Instruments DSC 220C under nitrogen atmosphere. Samples for DSC measurement were hermetically sealed in Al pans in the argon-filled glove box. The thermograms were recorded during a cooling scan (30 to -150°C) followed by a heating scan (-150 to 100°C), at a cooling and heating rate of $10^\circ\text{C min}^{-1}$. The data for phase transition temperatures, including melting temperatures (T_m), were taken at the peak maximum in the heating scans.

The thermal stabilities of G4 and $[\text{Li}(\text{G4})][\text{CTFSI}]$ were investigated using a Seiko Instruments thermogravimetry/differential thermal analyzer (TG/DTA 6200) from 30 to 500°C at a heating rate of $10^\circ\text{C min}^{-1}$ under nitrogen atmosphere, and their volatilities were measured using the thermal analyzer by maintaining their temperatures at 100°C for 3 h under nitrogen atmosphere.

The ionic conductivity of glyme–Li salt complexes was determined by performing complex impedance measurements using a computer-controlled Princeton Applied Research VMP2 potentiostat over a frequency range of 500 kHz– 1 Hz. A sample was placed in an air-tight glass vessel equipped with two platinum electrodes. Impedance measurements were performed at various temperatures. The temperature of the cell was cooled from 90 to 10°C

by using a programmable thermostated oven, and the samples were thermally equilibrated at each temperature for at least 2 h before the impedance measurements. Density measurement was performed by using a density/specific gravity meter DA-100 (Kyoto Electronics Manufacturing Co., Ltd.). Viscosity measurement was performed using a rheometer (Physica MCR301, Anton Paar) under dry atmosphere.

The self-diffusion coefficients of ions and solvents were determined by using pulsed gradient spin-echo nuclear magnetic resonance (PGSE-NMR). The detailed procedure of the PGSE-NMR measurements has been reported elsewhere [39–43]. The PGSE-NMR measurements were conducted by using a JEOL JNM-AL 400 spectrometer with a 9.4 T narrow bore superconducting magnet equipped with a JEOL pulse field gradient probe and a current amplifier. The self-diffusion coefficients were measured using the simple Hahn spin-echo sequence (i.e., $90^\circ - \tau - 180^\circ - \tau$ - acquisition), incorporating a sine gradient pulse in each τ period. The interval between two gradient pulses was set at 50 ms, and the duration of the field gradient was varied. The samples were inserted into a 5 mm (o.d.) NMR microtube (BMS-005J, Shigemi, Tokyo) in the glove box to a height of 5 mm, and the measurements for the glyme, lithium cation, and anion in $[\text{Li}(\text{G4})][\text{CTFSI}]$ were performed by examining ^1H , ^7Li , and ^{19}F nuclei, respectively, at 30°C .

The electrochemical stability of $[\text{Li}(\text{G4})][\text{CTFSI}]$ was evaluated by voltammetry using the Princeton Applied Research VMP2 potentiostat. Linear sweep voltammetry was carried out to evaluate the anodic limit by using a stainless steel electrode as working electrode and metallic lithium as reference/counter electrode in the two-electrode cell: $[\text{stainless steel}|\text{Li}(\text{G4})][\text{CTFSI}]/\text{Li metal}$. The electrode potential was swept from a rest potential to 6 V vs. Li/Li^+ at 30°C . Cyclic voltammetry was carried out to evaluate the cathodic stability by using a nickel electrode as the working electrode and metallic lithium as the reference/counter electrode in the two-electrode cell: $[\text{nickel}|\text{Li}(\text{G4})][\text{CTFSI}]/\text{Li metal}$. The electrode potential was swept for 10 cycles successively in the range of 2.4 to -0.5 V vs. Li/Li^+ at 30°C .

Galvanostatic charge–discharge measurements of the $[\text{LiCoO}_2][\text{Li}(\text{G4})][\text{CTFSI}]/\text{Li metal}$ anode cell were performed. The cathode layer, consisting of LiCoO_2 (85 wt%) as a cathode active material, acetylene black (9 wt%, Denki Kagaku Kogyo) as an electronically conductive additive, and poly(vinylidene fluoride) (PVDF, 6 wt%, Kureha Chemical) as a binder polymer, was coated onto an Al sheet. LiCoO_2 , acetylene black, and PVDF were mixed with *N*-methylpyrrolidone and thoroughly agitated in an agate mortar. The obtained paste was applied onto an Al current collector using an automatic applicator. After the paste was dried, the cathode sheet was cut into a circle shape (16 mm diameter, 50 μm thickness) and compressed to increase the packing density and improve the electronic conductivity. The cathode sheet, porous polypropylene separator (Celgard[®]3501, 25- μm thick), glyme–Li salt complex electrolyte, and lithium metal anode (Honjo Metal, 2 cm^2 area, 300 μm thick) were encapsulated into 2032-type coin cells. The charge–discharge test of the cell was performed in the voltage range of 3.0–4.2 V at a current density of 0.16 mA cm^{-2} (approximately 1/10 C) at 30°C .

3. Results and discussion

Fig. 2 shows the DSC heating traces for $[\text{Li}(\text{G3})][\text{CTFSI}]$ and $[\text{Li}(\text{G4})][\text{CTFSI}]$. The melting points of pure G3 ($T_m = -45^\circ\text{C}$) and pure G4 ($T_m = -30^\circ\text{C}$) were not observed in the DSC curves of both $[\text{Li}(\text{G3})][\text{CTFSI}]$ and $[\text{Li}(\text{G4})][\text{CTFSI}]$. This suggests that free glyme molecules do not exist in the equimolar mixtures. The melting points of $[\text{Li}(\text{G3})][\text{CTFSI}]$ and $[\text{Li}(\text{G4})][\text{CTFSI}]$ appeared at 71 and

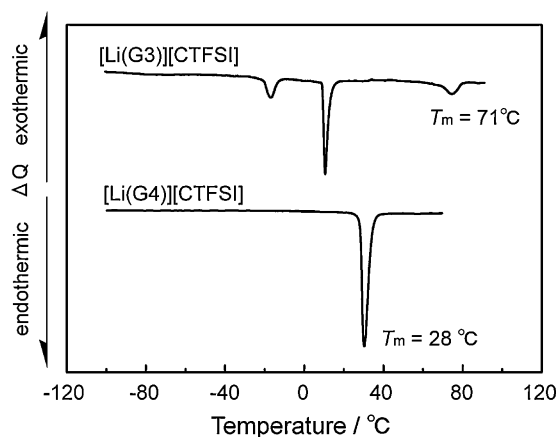


Fig. 2. DSC heating traces of [Li(G3)][CTFSI] and [Li(G4)][CTFSI] measured at a heating rate of $10^\circ\text{C min}^{-1}$.

28°C , respectively. The [Li(G3)][CTFSI] is a solid at room temperature. However, in the DSC trace of [Li(G3)][CTFSI], two solid–solid phase-transition temperatures (phase II to I: 11°C , phase III to II: -18°C) were observed. Indeed, phase I ($11^\circ\text{C} < T < 71^\circ\text{C}$) exhibits a relatively high ionic conductivity of 10^{-6} – $10^{-4} \text{ S cm}^{-1}$ (*vide infra*, Fig. 5). Although the melting point of [Li(G4)][CTFSI] was observed at 28°C , the complex maintains a liquid phase as supercooled liquid even below room temperature.

The thermal stability for [Li(G4)][CTFSI] was revealed by thermogravimetry (Fig. 3). In the case of pure G4, it starts to lose weight even from room temperature. G4 completely evaporates at around 200°C at this heating rate ($10^\circ\text{C min}^{-1}$), while the boiling point of G4 is 216°C . [Li(G4)][CTFSI] has good thermal stability and does not lose weight until 200°C . The evaporation of G4 from [Li(G4)][CTFSI] started at ca. 200°C , and G4 is completely removed from the complex at 385°C . Indeed, the 50% weight loss at 385°C in Fig. 3 agrees well with the content of G4 in the equimolar complex (47.1 wt%). The weight loss above 400°C is attributed to the decomposition of LiCTFSI. In order to evaluate the volatilities of pure G4 and [Li(G4)][CTFSI], the temperature of the samples was kept at 100°C for 3 h, as shown in Fig. 4. Pure G4 gradually loses weight, and ca. 50% of G4 evaporates within 3 h. On the other hand, [Li(G4)][CTFSI] exhibits negligible weight loss. This indicates that the vapor pressure of [Li(G4)][CTFSI] is negligible at temperatures lower than 100°C , and the equimolar mixture behaves like an RTIL.

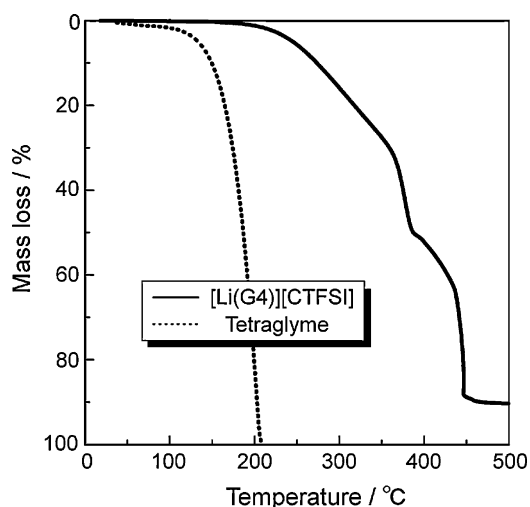


Fig. 3. Thermogravimetric curves of tetraglyme and [Li(G4)][CTFSI] measured at a heating rate of $10^\circ\text{C min}^{-1}$ under nitrogen atmosphere.

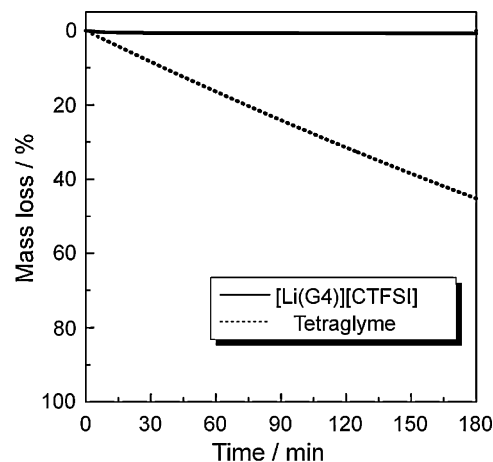


Fig. 4. Change in weight of tetraglyme and [Li(G4)][CTFSI] at 100°C for 3 h under nitrogen atmosphere.

Fig. 5 shows the temperature dependence of the ionic conductivity of [Li(G3)][CTFSI] and [Li(G4)][CTFSI]. The ionic conductivity of [Li(G3)][CTFSI] shows an inflection point at 70°C because of the liquid–solid phase transition. The melting point of [Li(G3)][CTFSI] is 71°C , as shown in Fig. 2. The ionic conductivity of the liquid phase [Li(G3)][CTFSI] ($71^\circ\text{C} < T$) is ca. $10^{-3} \text{ S cm}^{-1}$. Although [Li(G3)][CTFSI] is in solid state at a temperature lower than 71°C at equilibrium, [Li(G3)][CTFSI] exhibits ionic conductivity of $10^{-6} \text{ S cm}^{-1}$ even at room temperature. This suggests that the solid phase of the [Li(G3)][CTFSI] complex is an ionic conduction phase such as the plastic crystal phase. Another possibility arises from the slow crystallization kinetics of the liquid phase [Li(G3)][CTFSI], and the remaining liquid phase in the solid phase contributes to the ionic conduction in the cooling process. The [Li(G4)][CTFSI] complex is liquid in the temperature range of 25 – 200°C , as described before. The temperature dependency of the ionic conductivity of [Li(G4)][CTFSI] exhibits Vogel–Tamman–Fulcher (VTF) behavior, and the conductivity is $0.8 \times 10^{-3} \text{ S cm}^{-1}$ at 30°C .

The transport properties, viscosity (η), density (d), molar concentration (M), ionic conductivity (σ), diffusion coefficient (D), Li ion transference number (t_+), and ionicity ($\Lambda_{\text{imp}}/\Lambda_{\text{NMR}}$) [39–43], of [Li(G4)][CTFSI] at 30°C are summarized in Table 1. The self-diffusion coefficients of Li^+ cation (D_{cation}), [CTFSI] $^-$ anion (D_{anion}), and the G4 molecule (D_{sol}) can be evaluated by using the PGSE-NMR

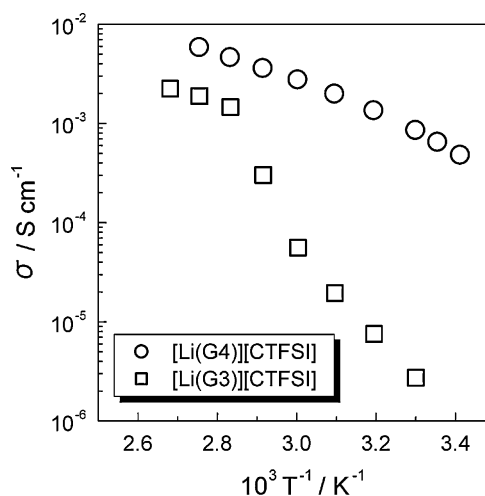


Fig. 5. Temperature dependence of ionic conductivity of [Li(G3)][CTFSI] and [Li(G4)][CTFSI].

Table 1
Physicochemical properties of [Li(G4)][CTFSI] at 30 °C.

	η (mPa s)	d (g cm ⁻³)	M (mol dm ⁻³)	σ (mS cm ⁻¹)	Diffusion coefficient ($\times 10^{-7}$ cm ² s ⁻¹)			t_+	$\Lambda_{\text{imp}}/\Lambda_{\text{NMR}}$
					D_{sol}	D_{cation}	D_{anion}		
[Li(G4)][CTFSI]	132.0	1.40	2.98	0.8	0.75	0.78	0.75	0.51	0.46

method for ⁷Li, ¹⁹F, and ¹H nuclei, respectively. The transference number of the Li⁺ cation is calculated from the diffusivity results ($t_+ = D_{\text{cation}}/(D_{\text{cation}} + D_{\text{anion}})$). The molar conductivity of [Li(G4)][CTFSI] is determined by using Eq. (1):

$$\Lambda_{\text{imp}} = \frac{\sigma}{c} \quad (1)$$

where c is the molar concentration of LiCTFSI. The molar conductivity (Λ_{NMR}) can also be calculated from the self-diffusion coefficients using the Nernst–Einstein equation (2):

$$\Lambda_{\text{NMR}} = \frac{N_A e^2 (D_{\text{cation}} + D_{\text{anion}})}{kT} = \frac{F^2 (D_{\text{cation}} + D_{\text{anion}})}{RT} \quad (2)$$

where N_A is Avogadro's number, e is the electric charge on each ionic carrier, k is Boltzmann's constant, F is the Faraday constant, and R is the gas constant. The molar conductivity based on the diffusivity (Λ_{NMR}) is higher than that based on ionic conductivity (Λ_{imp}). The $\Lambda_{\text{imp}}/\Lambda_{\text{NMR}}$ can be defined as the ionicity, in other words, dissociativity of the salt [39–43].

Although the viscosity of [Li(G4)][CTFSI] is approximately 10–100 times higher than that of typical organic electrolytes [44,45], the conductivity is close to 10⁻³ S cm⁻¹. This result comes from the high ionic concentration of the [Li(G4)][CTFSI] complex, reaching ca. 3 mol dm⁻³, as shown in Table 1. Each self-diffusion coefficient is on the order of 10⁻⁸ cm² s⁻¹ and is much smaller than that of typical organic electrolytes such as 1 M LiTFSI/propylene carbonate solution [44,45]. The self-diffusion coefficients of Li⁺ cation, the G4 molecule, and the anion are almost the same. In conventional aprotic organic electrolyte solutions, the diffusivity of the components generally follows the order: solvent > anion > Li⁺, because of the preferential solvation of Li⁺ by the solvent, resulting in the largest hydrodynamic volume among the components. Thus, the diffusivity behavior of the [Li(G4)][CTFSI] complex is completely different from that of conventional organic electrolyte solutions. One can assume that each Li⁺ cation is coordinated by a G4 molecule due to the Lewis acid (Li⁺ cation)/Lewis base (G4) interaction, as seen in crown ether complexes. These complex cations appear to diffuse together in the liquid. It would also be possible to consider a contact ion-pair formation between [Li(G4)]⁺ and [CTFSI]⁻ due to the similar diffusivity of Li⁺ cation, the G4 molecule, and the anion. However, this possibility is precluded by the high $\Lambda_{\text{imp}}/\Lambda_{\text{NMR}}$ value (Table 1). It should be noted that the $\Lambda_{\text{imp}}/\Lambda_{\text{NMR}}$ value, an indicator of the dissociativity, is ca. 0.5 though the concentration is very high (3 mol dm⁻³) and is comparable to those of conventional organic electrolyte solutions [46].

The transport properties, i.e., similar diffusivities of the Li⁺ cation, the G4 molecule, and the anion, a t_{Li} value close to 0.5, and a high $\Lambda_{\text{imp}}/\Lambda_{\text{NMR}}$ value, as well as a high thermal stability (Figs. 3 and 4) for [Li(G4)][CTFSI], are common characteristics of conventional RTILs [39–43]. The Lewis acidity of the Li⁺ cation is lowered by the coordination with the glyme, and the size of the cation becomes large by forming a complex cation [Li(G4)]⁺. The resulting [Li(G4)]⁺ cation can be regarded as a “soft Lewis acid.” Therefore, [Li(G4)][CTFSI] can be regarded as an RTIL consisting of a soft acid [Li(G4)]⁺ and a soft base [CTFSI]⁻. The formation of complex anions, such as BF₄⁻ and PF₆⁻, by Lewis acid/base reactions is well known, and such anions are widely used to form RTILs. However, the application of this concept for forming complex cations has not been reported. Here, we propose an approach for widen-

ing the materials composition of RTILs. An interesting characteristic of [Li(G4)][CTFSI] in terms of its application to LiBs is its high Li⁺-transference number (ca. 0.5), as shown in Table 1, which assures high Li⁺-conductivity. For the application of RTILs to LiBs as electrolytes, a methodology in which lithium salts are dissolved in electrochemically stable RTILs has been widely adopted [8–25]. In such cases, the optimum lithium salt concentration is rather low, because ionic conductivity of the RTIL solutions decreases with an increase in the lithium salt concentration due to a large increase in the viscosity of the solutions. As a result, the t_{Li} of such solutions is much smaller than 0.5. For instance, the t_{Li} values for *N*-alkyl-*N*-methylpyrrolidinium bis(trifluoromethanesulfonyl)imide/lithium salt mixtures applied to LiBs are reported to be ca. 0.1 [47].

Fig. 6 shows the linear sweep voltammograms of LiCTFSI/G4 mixtures measured at a scan rate of 1 mV s⁻¹ at 30 °C using stainless steel as the working electrode and lithium metal as the counter and reference electrode. In the case of the equimolar complex [Li(G4)][CTFSI], the anodic current starts to flow at ca. 4.5 V and rapidly increases from ca. 5.0 vs. Li/Li⁺. It is well known that the oxidation of ether compounds takes place at ca. 4 V vs. Li/Li⁺. Indeed, anodic current for the [Li(G4)₂₀][CTFSI] solution, where a large excess of G4 molecules exists (molar ratio of G4:LiCTFSI = 20:1), starts to flow from ca. 4 V. Free glyme molecules in the [Li(G4)₂₀][CTFSI] solution, which are not involved in the complexation with Li⁺, appear to be responsible for the lower oxidation limit. It is clear that the complex formation between Li⁺ and G4 enhances the oxidation stability of the ether structure. The distinct difference between the two mixtures in turn indicates that all of the G4 molecules in [Li(G4)][CTFSI] are complexed with Li⁺ cation.

Fig. 7 shows cyclic voltammograms of [Li(G4)][CTFSI] measured at a scan rate of 1 mV s⁻¹ at 30 °C using nickel metal as the working electrode and lithium metal as the counter and reference electrode. The cathodic current due to lithium deposition is observed at electrode potentials lower than 0 V vs. Li/Li⁺, and the stripping behavior appears in the returning anodic scan. The Li deposition/stripping can be repeated in [Li(G4)][CTFSI] for more than 10 cycles reversibly. This deposition/stripping behavior suggests that the glyme molecules are electrochemically stable even at 0 V. The complex cation [Li(G4)]⁺ is desolvated into free G4 and Li⁺ at the electrode interface, and the charge transfer process (i.e., Li deposi-

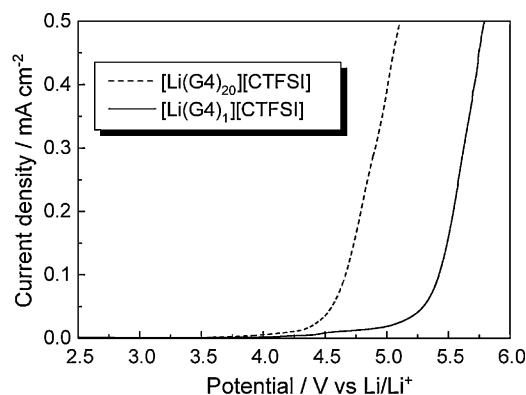


Fig. 6. Linear sweep voltammograms of [Li(G4)][CTFSI] and [Li(G4)₂₀][CTFSI] measured at a scan rate of 1 mV s⁻¹ at 30 °C. Stainless steel and lithium metal were used as the working electrode and the reference/counter electrode, respectively.

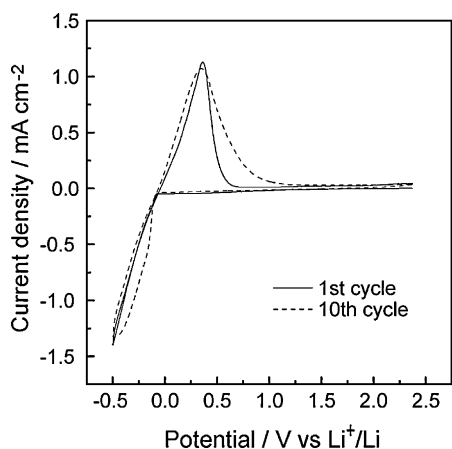


Fig. 7. Cyclic voltammogram (first cycle) of $[\text{Li}(\text{G4})][\text{CTFSI}]$ measured at a scan rate of 1 mV s^{-1} at 30°C . Nickel and lithium metal were used as the working electrode and the reference/counter electrode, respectively.

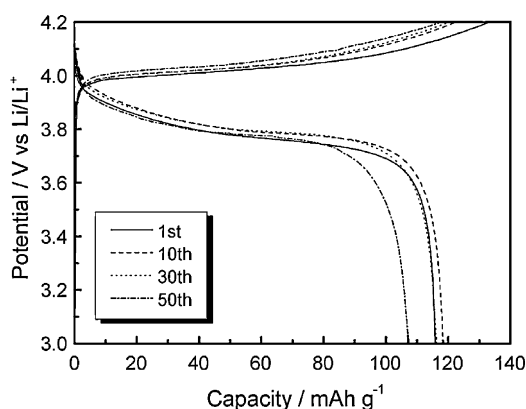


Fig. 8. Charge–discharge curves of a $[\text{LiCoO}_2][\text{Li}(\text{G4})][\text{CTFSI}]/\text{Li}$ metal cell. The charge–discharge test was performed at a current density of 0.16 mA cm^{-2} (approximately $1/10\text{C}$) at 30°C .

tion) takes place. The deposited Li is oxidized to form Li^+ , which is solvated again by G4 molecules. The formation and disruption of the ion–dipole interactions appear to be reversible at the interface.

Finally, the charge–discharge performance of a $[\text{LiCoO}_2][\text{Li}(\text{G4})][\text{CTFSI}]/\text{Li}$ metal cell was explored. The charge–discharge curves of the cell are shown in Fig. 8. The cell exhibited stable charge–discharge cycle behavior for over 50 cycles. The first charge and discharge capacities are 132 and 120 mAh g^{-1} , respectively, which are close to the theoretical capacity of Li_xCoO_2 (140 mAh g^{-1} , $0.5 < x < 1$). The coulombic efficiency of the first cycle was 87%, however, the charge–discharge reversibility was improved after the 2nd cycle, and the efficiency became higher than 95%. The discharge capacity of 108 mAh g^{-1} is retained even after 50 cycles, suggesting that considerable degradation of the electrolyte does not take place during the repetition of the charge and discharge. This result agrees with the results of electrochemical stability (Figs. 6 and 7) of $[\text{Li}(\text{G4})][\text{CTFSI}]$. The equimolar complex $[\text{Li}(\text{G4})][\text{CTFSI}]$ is proved to be applicable to the 4 V class cathode at room temperature.

4. Conclusion

In this paper, we explored the possibility of glyme–Li salt complexes as new liquid electrolytes for LiBs. Triglyme (G3) and tetraglyme (G4) form 1:1 complexes with LiCTFSI : $[\text{Li}(\text{G3})][\text{CTFSI}]$ and $[\text{Li}(\text{G4})][\text{CTFSI}]$, respectively. $[\text{Li}(\text{G4})][\text{CTFSI}]$ is a liquid, whereas $[\text{Li}(\text{G3})][\text{CTFSI}]$ is a solid at room temperature. The thermal

stability of $[\text{Li}(\text{G4})][\text{CTFSI}]$ is much higher than that of pure G4, and the vapor pressure of $[\text{Li}(\text{G4})][\text{CTFSI}]$ is negligible at temperatures lower than 100°C . The transport properties of $[\text{Li}(\text{G4})][\text{CTFSI}]$ are characterized by relatively high ionic conductivity of ca. 1 mS cm^{-1} at 30°C , which is caused by a high salt concentration of ca. 3 M, although the diffusion of Li^+ and CTFSI anion is slow (ca. $10^{-7} \text{ cm}^2 \text{ s}^{-1}$ at 30°C). The same diffusivity of Li^+ and G4 and a high $A_{\text{imp}}/A_{\text{NMR}}$ (ionicity) value of 0.5 indicate that $[\text{Li}(\text{G4})][\text{CTFSI}]$ consists of the complex cation, $[\text{Li}(\text{G4})]^+$, and CTFSI anion. $[\text{Li}(\text{G4})][\text{CTFSI}]$ is electrochemically stable within the electrode potential range of 0–4.5 V vs. Li/Li^+ . $[\text{Li}(\text{G4})][\text{CTFSI}]$ exhibits much better oxidative stability than $[\text{Li}(\text{G4})_{20}][\text{CTFSI}]$, which contains a large number of free G4 molecules. A $[\text{LiCoO}_2][\text{Li}(\text{G4})][\text{CTFSI}]/\text{Li}$ metal cell exhibits stable charge–discharge cycle behavior for over 50 cycles, indicating that the $[\text{Li}(\text{G4})][\text{CTFSI}]$ complex is applicable to a 4 V class LiB.

Glyme–Li salt equimolar complexes appear to be a new class of RTILs, which consist of a complex cation $[\text{Li}(\text{glyme})]^+$ and an anion and may be able to enhance the safety of LiBs when used as the electrolyte. A large number of glyme–Li salt complexes can be prepared from different glymes and Li salts. The chemical structure of glyme molecules can be easily modified, which will affect the physicochemical properties of the glyme–Li salt equimolar complexes. Further investigations are under way in our group and will be reported in due course.

Acknowledgments

This study was supported in part by Technology Research Grant Program from the New Energy and Industrial Technology Development Organization (NEDO) of Japan and by a Grant-in-Aid for Scientific Research from the MEXT of Japan in the priority area “Science of Ionic Liquids” (#452-17073009).

References

- [1] T. Tanaka, K. Ohta, N. Arai, J. Power Sources 97–98 (2001) 2.
- [2] T. Takamura, Solid State Ionics 152–153 (2002) 19.
- [3] K. Zaghbi, P. Charest, A. Guerfi, J. Shim, M. Perrier, K. Striebel, J. Power Sources 134 (2004) 124.
- [4] S. Seki, Y. Kobayashi, H. Miyashiro, A. Usami, Y. Mita, N. Terada, J. Electrochem. Soc. 153 (2006) A1073.
- [5] M. Watanabe, T. Endo, A. Nishimoto, K. Miura, M. Yanagida, J. Power Sources 81–82 (1999) 786.
- [6] E. Paillard, C. lojoiu, F. Alloin, J. Guindet, J.-Y. Sanchez, Electrochim. Acta 52 (2007) 3758.
- [7] R. Kanno, M. Murayama, J. Electrochem. Soc. 148 (2001) A742.
- [8] D.R. MacFarlane, P. Meakin, J. Sun, N. Amini, M. Forsyth, J. Phys. Chem. B 103 (1999) 4164.
- [9] D.R. MacFarlane, J. Sun, J. Golding, P. Meakin, M. Forsyth, Electrochim. Acta 45 (2000) 1271.
- [10] H. Matsumoto, M. Yanagida, K. Tanimoto, M. Nomura, Y. Kitagawa, Y. Iyazaki, Chem. Lett. (2000) 922.
- [11] H. Matsumoto, T. Matsuda, Y. Miyazaki, Chem. Lett. (2000) 1430.
- [12] H. Sakaebe, H. Matsumoto, K. Tatsumi, Electrochim. Acta 53 (2007) 1048.
- [13] H. Sakaebe, H. Matsumoto, K. Tatsumi, J. Power Sources 146 (2005) 693.
- [14] S. Seki, Y. Kobayashi, H. Miyashiro, Y. Mita, A. Usami, M. Watanabe, Electrochem. Solid-State Lett. 8 (2005) A577.
- [15] S. Seki, Y. Kobayashi, H. Miyashiro, Y. Ohno, A. Usami, Y. Mita, N. Kihira, M. Watanabe, N. Terada, J. Phys. Chem. B 110 (2006) 10228.
- [16] S. Seki, Y. Kobayashi, H. Miyashiro, Y. Ohno, A. Usami, Y. Mita, M. Watanabe, N. Terada, Chem. Commun. (2006) 544.
- [17] S. Seki, Y. Ohno, H. Miyashiro, Y. Kobayashi, A. Usami, Y. Mita, N. Terada, K. Hayamizu, S. Tsuzuki, M. Watanabe, J. Electrochem. Soc. 155 (2008) A421.
- [18] K. Hayamizu, S. Tsuzuki, S. Seki, Y. Ohno, H. Miyashiro, Y. Kobayashi, J. Phys. Chem. B 112 (2008) 1189.
- [19] S. Seki, Y. Kobayashi, H. Miyashiro, Y. Ohno, Y. Mita, N. Terada, P. Charest, A. Guerfi, K. Zaghbi, J. Phys. Chem. C 112 (2008) 16708.
- [20] Q. Zhou, W.A. Henderson, G.B. Appetecchi, M. Montanino, S. Passerini, J. Phys. Chem. B 112 (2008) 13577.
- [21] G.B. Appetecchi, M. Montanino, A. Balducci, S.F. Lux, M. Winter, S. Passerini, J. Power Sources 192 (2009) 599.
- [22] M. Ishikawa, T. Sugimoto, M. Kikuta, E. Ishiko, M. Kono, J. Power Sources 162 (2006) 658.

- [23] T. Sugimoto, Y. Atsumi, M. Kikuta, E. Ishiko, M. Kono, M. Ishikawa, J. Power Sources 189 (2009) 802.
- [24] A. Fernicola, F. Croce, B. Scrosati, T. Watanabe, H. Ohno, J. Power Sources 174 (2007) 342.
- [25] A. Martinelli, A. Matic, P. Jacobsson, L. Börjesson, A. Fernicola, B. Scrosati, J. Phys. Chem. B 113 (2009) 11247.
- [26] M. Ue, M. Takeda, T. Takahashi, M. Takehara, Electrochem. Solid-State Lett. 5 (2002) A119.
- [27] M. Ue, M. Takeda, A. Toriumi, A. Kominato, R. Hagiwara, Y. Ito, J. Electrochem. Soc. 150 (2003) A499.
- [28] Y.-J. Kim, Y. Matsuzawa, S. Ozaki, K.C. Park, C. Kim, M. Endo, H. Yoshida, G. Masuda, T. Sato, M.S. Dresselhaus, J. Electrochem. Soc. 152 (2005) A710.
- [29] D. Kuang, P. Wang, S. Ito, S.M. Zakeeruddin, M. Gratzel, J. Am. Chem. Soc. 128 (2006) 7732.
- [30] R. Kawano, H. Matsui, C. Matsuyama, A. Sato, M.A.B.H. Susan, N. Tanabe, M. Watanabe, J. Photochem. Photobiol. A: Chem. 164 (2004) 87.
- [31] A. Noda, M.A.B.H. Susan, K. Kudo, S. Mitsushima, K. Hayamizu, M. Watanabe, J. Phys. Chem. B 107 (2003) 4024.
- [32] H. Nakamoto, A. Noda, K. Hayamizu, S. Hayashi, H. Hamaguchi, M. Watanabe, J. Phys. Chem. C 111 (2007) 1541.
- [33] H. Nakamoto, M. Watanabe, Chem. Commun. (2007) 2539.
- [34] T. Yasuda, A. Ogawa, M. Kanno, K. Mori, K. Sakakibara, M. Watanabe, Chem. Lett. 38 (2009) 692.
- [35] W.A. Henderson, N.R. Brooks, W.W. Brennessel, V.G. Young Jr., Chem. Mater. 15 (2003) 4679.
- [36] W.A. Henderson, N.R. Brooks, V.G. Young Jr., Chem. Mater. 15 (2003) 4685.
- [37] W.A. Henderson, J. Phys. Chem. B 110 (2006) 13177.
- [38] M. Nakamura, Y. Kazue, S. Seki, K. Dokko, M. Watanabe, Glyme–Li TFSI Complex as Electrolytes for Lithium Secondary Batteries, Presented at the 214th ECS Meeting, Honolulu, HI, 2008, #742.
- [39] A. Noda, K. Hayamizu, M. Watanabe, J. Phys. Chem. B 105 (2001) 4603.
- [40] H. Tokuda, K. Hayamizu, K. Ishii, M.A.B.H. Susan, M. Watanabe, J. Phys. Chem. B 108 (2004) 16593.
- [41] H. Tokuda, K. Hayamizu, K. Ishii, M.A.B.H. Susan, M. Watanabe, J. Phys. Chem. B 109 (2005) 6103.
- [42] H. Tokuda, K. Ishii, M.A.B.H. Susan, K. Hayamizu, M. Watanabe, J. Phys. Chem. B 110 (2006) 2833.
- [43] H. Tokuda, S. Tsuzuki, M.A.B.H. Susan, K. Hayamizu, M. Watanabe, J. Phys. Chem. B 110 (2006) 19593.
- [44] G. Pistoia, M. De Rossi, B. Scrosati, J. Electrochem. Soc. 117 (1970) 500.
- [45] S. Kinoshita, M. Kotato, Y. Sakata, M. Ue, Y. Watanabe, H. Morimoto, S. Tobishima, J. Power Sources 183 (2008) 755.
- [46] K. Hayamizu, Y. Aihara, S. Arai, C.G. Martinez, J. Phys. Chem. B 103 (1999) 519.
- [47] T. Frömling, M. Kunze, M. Schönhoff, J. Sundermeyer, B. Roling, J. Phys. Chem. B 112 (2008) 12985.